Am J Cancer Res 2016;6(11):2489-2501
www.ajcr.us /ISSN:2156-6976/ajcr0042521

Original Article

The role of PIM1 in the ibrutinib-resistant ABC subtype of diffuse large B-cell lymphoma

Hsu-Ping Kuo, Scott A Ezell, Sidney Hsieh, Karl J Schweighofer, Leo WK Cheung, Shiquan Wu, Mutiah Apatira, Mint Sirisawad, Karl Eckert, Yu Liang, Jeff Hsu, Chun-Te Chen, Darrin Beaupre, Betty Y Chang

Department of Research, Pharmacyclics, LLC, an AbbVie Company, Sunnyvale, CA, USA

Received October 18, 2016; Accepted October 24, 2016; Epub November 1, 2016; Published November 15, 2016

Abstract: Diffuse large B cell lymphoma (DLBCL) is a heterogeneous lymphoma and the most common subtype of non-Hodgkin lymphoma, accounting for roughly 30% of newly diagnosed cases in the United States. DLBCL can be separated into the activated B cell-like (ABC) and germinal center B cell-like (GCB) subtypes, with distinct gene expression profiles, oncogenic aberrations, and clinical outcomes. ABC-DLBCL is characterized by chronically active B-cell receptor (BCR) signaling that can be modulated by Bruton's tyrosine kinase (BTK) activity. Thus, BTK serves as an attractive therapeutic target in this type of B-cell malignancy. Ibrutinib, a first-in-class, orally available covalent BTK inhibitor, has demonstrated clinical activity in several B-cell leukemias and lymphomas. A phase 1/2 clinical trial of single-agent ibrutinib in relapsed and refractory DLBCL patients revealed an overall response rate of 37% in ABC-DLBCL patients. However, responses to kinase-directed therapies are often limited by emerging resistance mechanisms that bypass the therapeutic target. Here we report the discovery of point mutations within the kinase PIM1 that reduce sensitivity to ibrutinib in ABC-DLBCL. These mutations stabilize PIM1 and affect upstream regulators and downstream targets of NF-κB signaling. The introduction of mutant PIM1 into an ABC-DLBCL cell line, TMD8, increased colony formation and decreased sensitivity to ibrutinib. In addition, ibrutinib-resistant cell lines generated by prolonged ibrutinib exposure *in vitro* upregulated PIM1 expression, consistent with a role for PIM1 in antagonizing ibrutinib activity. The combination of a pan-PIM inhibitor with ibrutinib synergistically inhibited proliferation *in vitro* and tumor growth *in vivo*. Together, these data provide a rationale for combining BTK and PIM1 inhibition in the treatment of ABC-DLBCL.

Keywords: Bruton's tyrosine kinase, ibrutinib, DLBCL, PIM1

Introduction

Bruton's tyrosine kinase (BTK) is critical for B-cell development, proliferation, and survival. BTK was identified through the occurrence of inactivating *BTK* mutations in X-linked agammaglobulinemia, a rare disorder characterized by a lack of mature B cells and markedly reduced immunoglobulins [1]. Recent work has determined that BTK also plays a critical role in certain B-cell leukemias and lymphomas [2-5], leading to the development of ibrutinib, a first-in-class covalent inhibitor of BTK [6]. Ibrutinib acts by preventing the activation of NF-κB signaling downstream of the B-cell receptor (BCR), a process that requires phosphorylation of phospholipase C gamma (PLCγ) by BTK [7]. Ibrutinib is approved for the treatment of patients with chronic lymphocytic leukemia, including those with deletion 17p, patients with mantle cell lymphoma (MCL) who have received at least one prior therapy, and those patients with Waldenström's macroglobulinemia. Ibrutinib is also active against a subset of activated B cell-like (ABC) diffuse large B-cell lymphoma (ABC-DLBCL), many of which carry mutations in BCR components and *MYD88* [8]. However, additional modifiers of ibrutinib sensitivity likely exist in ABC-DLBCL, and identifying them is key to selecting patients to receive this therapy.

Serine/threonine kinases of the proviral insertion in murine (PIM) family are critical regulators of turmorigenesis in a number of hematologic malignancies and solid cancers [9, 10]. The role of PIM1 in oncogenic processes is best characterized when comparing it with other PIM family

members that are involved in the regulation of survival, cell cycle, transcription, translation, and drug resistance [11]. PIM1 is commonly overexpressed in human cancers, and its expression is correlated with poor prognosis in leukemias [12], MCL [13], and DLBCL [14]. Therefore, PIM1 is emerging as an attractive drug target for cancer therapy [15]. However, the fact that PIM family members can compensate for each other to generate lymphomas underscores their potential redundancy in oncogenesis. Indeed, similar to the function of PIM1 on mTOR regulation [16], PIM2 has been identified as a key oncogenic signaling node in ABC-DLBCL that controls mTOR pathway activity [17]. The attribution of oncogenic activity to PIM isoforms argues for the development of pan-PIM inhibitors targeting all family members [18].

Here, we report that mutations in *PIM1* are associated with intrinsic ibrutinib resistance in ABC-DLBCL. Introducing one of these mutations into an ABC-DLBCL cell line is sufficient to induce ibrutinib resistance. Mutations in *PIM1* appear to stabilize the protein and enhance NF-κB signaling. Our data suggest that the combination of pan-PIM inhibitors with ibrutinib results in greater efficacy than ibrutinib as a single agent and can circumvent resistance.

Methods

Cell culture

The ABC-DLBCL cell lines TMD8 and HBL1 (gifts from Dr. Daniel Krappmann, German Research Center for Environmental Health, Neuherberg, Germany) were grown to log phase at 37°C in the presence of 5% CO_2. The cells were cultured in RPMI 1640 medium (Thermo Fisher Scientific) with 10% FBS (Atlanta Biologicals), 1 mM sodium pyruvate (Thermo Fisher Scientific), and 1% Pen/Strep (Thermo Fisher Scientific). Ibrutinib-resistant HBL1 and TMD8 cells were generated by *in vitro* culture of the parental cell lines for prolonged periods of time with progressively increasing concentrations of ibrutinib. TMD8 (PIM1-WT), TMD8 (PIM1-L2V), TMD8 (PIM1-P81S), and TMD8 (PIM1-S97N) were generated by introducing wild-type (WT) PIM1 or 1 of 3 mutants, PIM1 (L2V), PIM1 (P81S), or PIM1 (S97N), into the TMD8 cell line. HEK 293T cells were cultured in DMEM medium (Thermo Fisher Scientific) with 10% FBS (Atlanta Biologicals) and 1% Pen/Strep (Thermo Fisher Scientific).

Reagents and antibodies

Cycloheximide (C4859-1ML) was purchased from Sigma-Aldrich. Antibodies against PIM1 (ab54457) and β-actin (3700S) were obtained from Abcam and Cell Signaling Technology, respectively. AZD-1208 (S7104) was purchased from Selleckchem.

Cell viability assays

CellTiter-Glo® luminescent cell viability assays (Promega) were performed according to the manufacturer's instructions. Briefly, cells were seeded at 8,000-10,000 cells/well in a 96-well plate in the presence of single drugs or drug combinations for 3 days. The number of viable cells in culture was determined by quantification of the presence of ATP, which was proportional to luminescent signal detected. The combination index (CI), a drug interactivity measurement, was calculated with CalcuSyn software (Biosoft), as described previously [19, 20]. Synergy scores and isobolograms were generated by the Chalice Analyzer (Horizon CombinatoRx). A dose matrix was used to evaluate the combination effect. The isobologram determines the reduction in drug concentration required to achieve the desired effect in combination compared with the single-agent doses.

RT-PCR assays

The TaqMan® Fast Cells-to-C_T™ Kit (Life Technologies) was used to extract total RNA and reverse transcribe (RT) RNA to cDNA according to the manufacturer's specifications. Four microliters of cDNA from the RT reaction was used to set up the TaqMan® Quantitative RT-PCR on a QuantStudio™ 7 Flex Real-Time PCR System (Life Technologies). The TaqMan® Gene Expression Assays used for this study include PIM1 (Hs01065498_m1), PIM2 (Hs00179139_m1), PIM3 (Hs00420511_g1), GAPDH (Hs02758991_g1), and ACTB (Hs01060665_g1).

Xenograft study

All animal studies were completed under Institutional Animal Care and Use Committee (IACUC)-approved protocols for animal welfare. CB17 SCID mice (ENVIGO) were subcutaneously inoculated with 3×10^6 HBL1 cells in a suspension containing Matrigel (Corning). When

tumors reached approximately 150 mm^3 (14 days after tumor inoculation), mice were randomly assigned and treated once daily with ibrutinib (24 mg/kg), AZD-1208 (10 mg/kg), or a drug combination by oral gavage with 9 mice per group. Tumor volume was measured twice weekly and calculated as tumor volume = (length × $width^2$) × 0.5 according to a previously described method [21].

Colony formation assays

Cells (1,000 or 3,000 cells/well) were suspended in 0.9% methylcellulose (MethoCult™ H4100, STEMCELL Technologies) containing culture medium, and 0.3 mL of the mixture was plated in each well of 24-well culture plates. The colonies were counted on day 7. HBL1 cells were treated with vehicle, ibrutinib, AZD-1208, or the combination. WT or mutant *PIM1*-transduced TMD8 cells were treated with vehicle or ibrutinib.

Protein stability assays

HEK 293T cells were transiently transfected with WT *PIM1* or one of 3 mutants, *PIM1 (L2V)*, *PIM1 (P81S)*, or *PIM1 (S97N)*. Forty-eight hours after transfection, 100 μg/mL of cycloheximide was added to block protein synthesis. Cellular proteins were harvested at different time points after cycloheximide treatment, and PIM1 protein level was detected by western blot. PIM1 protein level in the cells collected at time 0 hour was defined as 1.0.

Western blot

Cells were washed with phosphate-buffered saline and lysed with RIPA buffer (R0278, Sigma-Aldrich) containing protease inhibitor cocktail (05892791001, Sigma-Aldrich) on ice. Cell debris was removed by centrifugation at 13,000 rpm at 4°C for 10 minutes. Cell lysates were subjected to SDS-PAGE separation and subsequently transferred onto a polyvinylidene difluoride membrane (IPFL00010, Millipore). The membranes were incubated with Odyssey Blocking Buffer (927-40000, LI-COR Biosciences) and were probed with various primary antibodies. After extensive washing, the membranes were incubated with IRDye®800CW- or IRDye®680RD-conjugated secondary antibodies and detected by LI-COR Odyssey Imaging System.

Gene expression analyses and statistics

GeneChip® Human Transcriptome Array 2.0 (HTA 2.0, Affymetrix) was used to analyze gene expression of parental TMD8 and ibrutinib-resistant TMD8 cells. RNA-Seq with minimum of 50 million paired-end reads per sample and the Cancer ACE Transcriptome analysis (Personalis) was used to study the gene expression of WT or mutant PIM1-transduced TMD8 cells. Gene set enrichment analyses (GSEA) were performed using GSEA v2.2.2 software (http://www.broad.mit.edu/gsea) with 1,000 data permutations. Enriched gene sets are selected based on statistical significance (FDR q-value <0.25 and normalized *p*-value <0.05).

Gene expression of formalin-fixed paraffin-embedded (FFPE) specimens from the phase 2 PCYC-1106 trial (NCT01325701) was analyzed using GeneChip® Human Genome U133 Plus 2.0 Array (Affymetrix) and data were normalized using the robust multiarray average (RMA) algorithm. Subtypes of DLBCL were identified based on the classification algorithm [22]. A test for differential expression of genes between ABC-DLBCL responders (complete response + partial response [CR + PR]) and non-responders (stable disease + progressive disease [SD + PD]) to ibrutinib was performed using the rank product statistics (RankProd R package).

Mutation analyses

PIM1 mutational analysis was performed with baseline clinical tumor biopsy samples from 2 studies, PCYC-04753 (NCT00849654) and PCYC-1106 (NCT01325701). Based on gene expression data, we used OmicSoft Array Studio's classification module to build linear discriminant analysis (LDA) model/classifier and neural networks of different model sizes. Model assessment was performed using a 5-fold cross-validation procedure, and LDA was selected for final GEP classification of DLBCL subtypes. A batch correction was applied to the data within Array Studio. Sequencing was performed using the FoundationOne Heme™ panel following the validated next-generation sequencing (NGS)-based protocol to interrogate complete DNA coding sequences of 405 genes, as well as selected introns of 31 genes involved in rearrangements. RNA sequences of 265 commonly rearranged genes were ana-

A

Patient	PIM1 mutations	Subtype	Clinical response
1	G28D	ABC	CR
2	G28D	ABC	PD
3	M1I, L2F, E32K, P33fs*68, Q37H, H68D, E70Q, P81S, E89K, V90L, S97N, Q127*, E135Q, E142fs*132, H165Y,	ABC	PD
4	L2V	ABC	PD
5	P81S	ABC	PD
6	M1I, P16S, C17S, G28V, K29N, K29fs*18, E30K, Q37H, G55D, I66M, E70Q, P81A, P87T, V90fs*27, L93V, S97T, P125S, V126M, E171K, L174F, I175V, E181D, L184F, L193F	GCB	SD

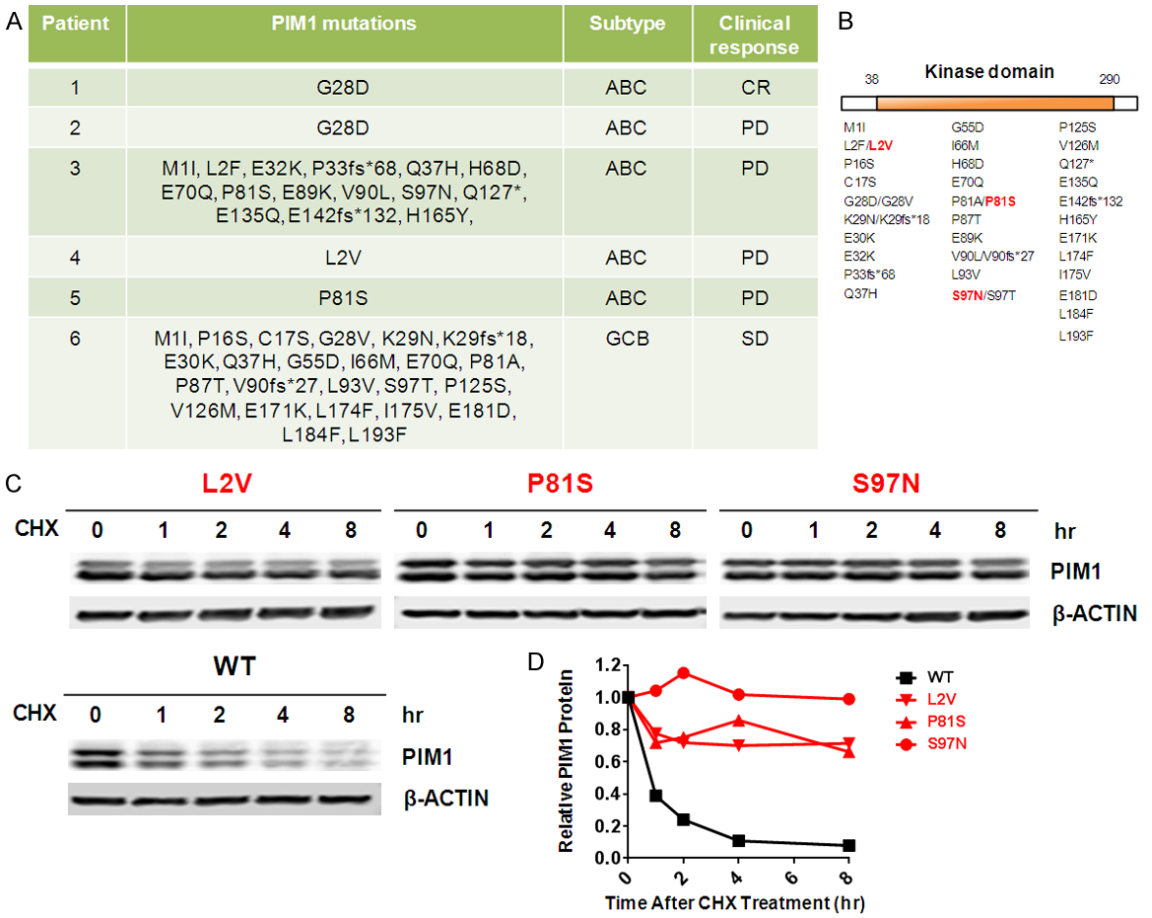

Figure 1. PIM1 mutations identified in patients with poor responses to ibrutinib increased protein stability. A. Mutation sites of PIM1 identified in ABC- and GCB-DLBCL patient samples. B. Representation of the PIM1 protein showing localization of the mutations observed. C. HEK 293T cells were transiently transfected with WT or mutant *PIM1* (L2V, P81S, S97N) constructs, treated with cycloheximide (CHX), and harvested at the indicated time points for immunoblot analysis with anti-PIM1 or anti-β-actin antibodies. D. Semi-quantification using β-actin as a loading control and relative PIM1 levels at time 0 hour as 1.0 were used to determine protein stability.

lyzed to identify gene fusions. A subgroup of samples was analyzed on earlier versions of the FoundationOne Heme™ panels, where only DNA was extracted and sequenced. Sequence data were processed and analyzed for base substitutions, insertions, deletions, copy-number alterations, and selected gene fusions [23].

Results

PIM1 mutations were more frequent in ABC-DLBCL patients

To understand the genetic basis of primary ibrutinib resistance in DLBCL, we profiled the genomes of baseline tumor biopsies from patients using the FoundationOne Heme™ panel following a validated NGS-based protocol. We identified several dozen mutations in *PIM1*, which encodes a serine/threonine kinase that has been implicated in DLBCL tumorigenesis [24]. Interestingly, in 48 DLBCL patient samples with available genomic profiling, *PIM1* mutations appeared more frequently in patients diagnosed with ABC-DLBCL than those diagnosed with germinal center B cell–like (GCB)-DLBCL (5 of 6 DLBCL patients with *PIM1* mutations had ABC-DLBCL). Four of these 5 patients (80%) with ABC-DLBCL containing *PIM1* mutations exhibited a poor clinical response (PD + SD) to ibrutinib. In comparison, only 13 of 26 (50%) ABC-DLBCL patients without *PIM1* mutations exhibited a poor response to ibrutinib (**Figure 1A**), suggesting that these mutations may be involved in primary resistance to ibrutinib. We selected mutations exclusively associated with patients who had pro-

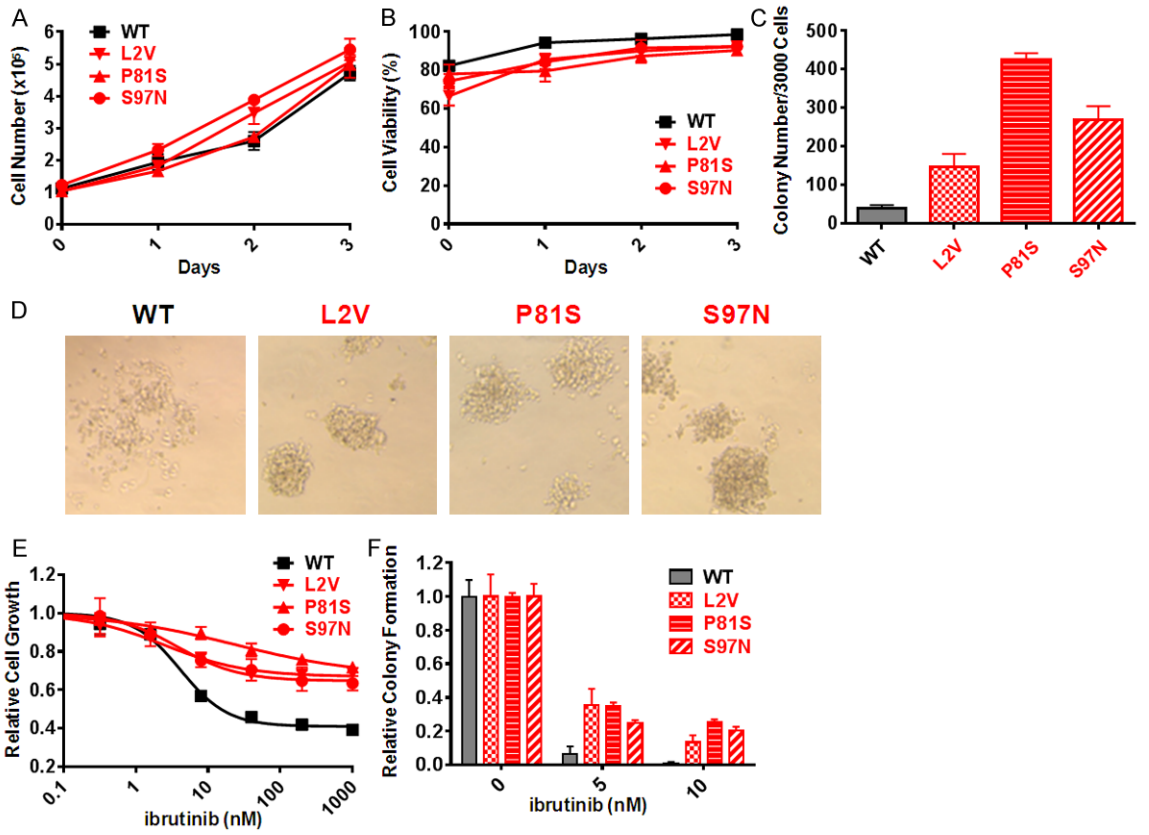

Figure 2. Mutant *PIM1*-transduced TMD8 cells had increased colony formation and were more resistant to ibrutinib treatment. (A) WT or mutant *PIM1*-transduced TMD8 cells were plated at 1×10^5 per well, and cell number was counted at indicated time points. (B) WT or mutant *PIM1*-transduced TMD8 cells were plated as in (A) and trypan blue exclusion was used to detect cell viability. (C) WT or mutant *PIM1*-transduced TMD8 cells were plated in 0.9% MethoCult (3,000 cells/well), and colony formation was scored after 7 days. Graphs represent quantifications of 3 wells, expressed as mean ± SD. (D) Photomicrographs of typical colonies generated by WT or mutant *PIM1*-transduced TMD8 cells. (E) WT or mutant *PIM1*-transduced TMD8 cells were treated with indicated concentrations of ibrutinib for 3 days, and the drug effect on cell growth was determined by CellTiter-Glo Luminescent Cell Viability Assay. (F) WT or mutant *PIM1*-transduced TMD8 cells were plated in 0.9% MethoCult (3,000 cells/well) with indicated concentrations of ibrutinib, and colony formation was scored after 7 days. Graphs represent quantifications of 3 wells and normalizations to the vehicle-treated samples.

gressed during ibrutinib treatment for further analysis. Specifically, we focused on three PIM1 point mutations: L2V, P81S, and S97N (**Figure 1B**).

PIM1 mutations identified in patients with poor response to ibrutinib increased protein stability

We cloned and expressed each PIM1 variant, as well as the WT protein, in HEK 293T cells. Cycloheximide treatment demonstrated that the PIM1-mutant cells all have significantly greater half-lives than those that express WT PIM1 (>8 hours, versus approximately 1 hour for WT) (**Figure 1C** and **1D**).

Mutant PIM1-expressing TMD8 cells had increased colony formation and were more resistant to ibrutinib treatment

Expression of the PIM1 mutants in TMD8 cells did not significantly alter basal proliferation rate or viability (**Figure 2A** and **2B**). However, the mutants did greatly affect colony morphology and increase colony number when cells were plated in methylcellulose substrate (**Figure 2C** and **2D**), suggesting that the tumorigenic potential of TMD8 is increased by mutations in PIM1. In addition, *in vitro* sensitivity to ibrutinib was significantly decreased by the mutations (EC_{50} of ibrutinib in TMD8 cells expressing WT PIM1 was 47 nM, and EC_{50}s in

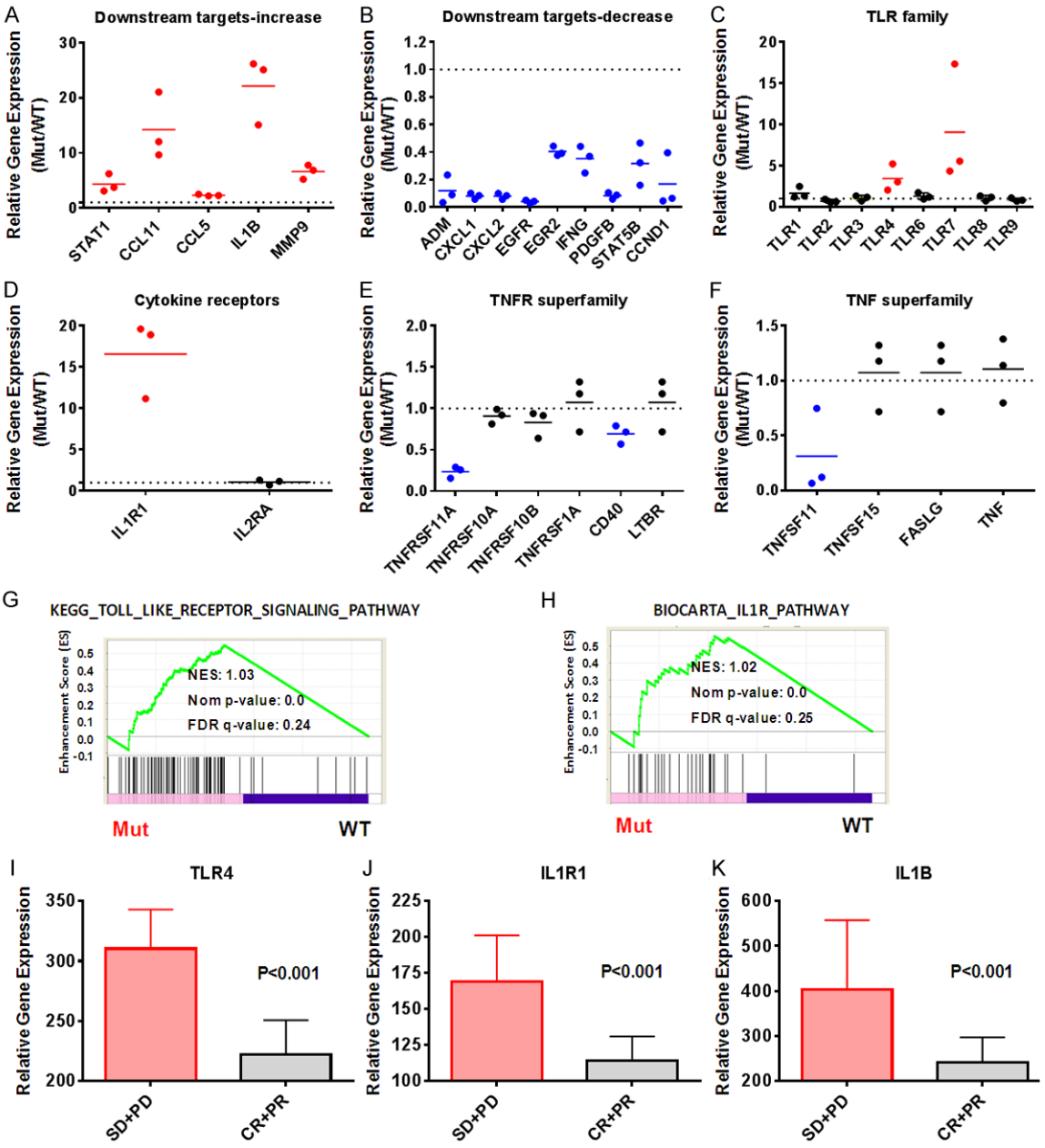

Figure 3. PIM1 mutations affected gene expression levels of upsteam regulators and downstream targets of the NF-κB pathway. (A-F) TaqMan® Array Human NF-κB Pathway was used to analyze the expression levels of the indicated genes. *GAPDH*, *HPRT1*, *GUSB*, and *18S* were used as internal controls. Relative gene expression indicates the ratio of average gene expression in PIM1-L2V, PIM1-P81S, and PIM1-S97N cells to WT PIM1-expressing cells. Gene expression of downstream targets is shown in (A, B), while gene expression of upstream regulators in NF-κB signaling pathways is shown in (C-F). (G, H) GSEA analyses demonstrate that the expression of genes associated with the Toll-like receptor (TLR) signaling pathway (G) and the IL-1 receptor (IL1R) pathway (H) is enriched in mutant *PIM1*-transduced TMD8 cells compared with WT *PIM1*-transduced cells. (I-K) Higher gene expression levels of TLR4 (I), IL1R1 (J), and IL1B (K) were detected in the tumors from ABC-DLBCL patients with poorer responses to ibrutinib (SD + PD). A rank-based statistic (RankProd) was used to determine the significance (P<0.001).

TMD8 cells expressing each of the three mutant PIM1 were greater than 1,000 nM) (**Figure 2E**), demonstrating that mutation of PIM1 is sufficient to create an ibrutinib-resistant phenotype. TMD8 lines expressing any of the mutant PIM1 isoforms also formed more colonies than WT PIM1 while exposed to ibrutinib (**Figure 2F**).

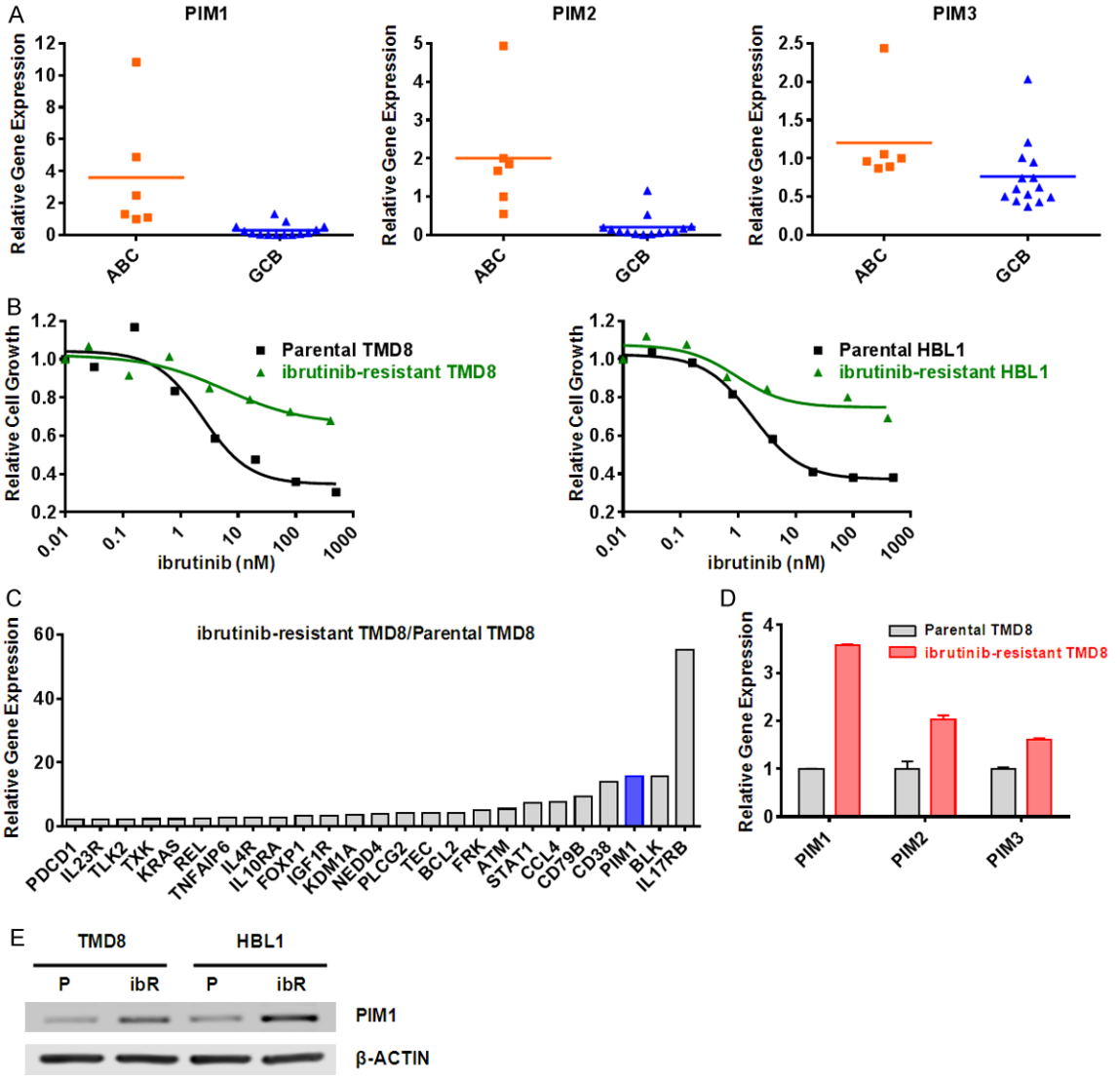

Figure 4. Ibrutinib-resistant ABC-DLBCL cells had higher *PIM1* expression levels. A. ABC-DLBCL cell lines had higher gene expression levels of *PIM1*, *PIM2*, and *PIM3*. ABC-DLBCL cell lines (TMD8, HBL1, OCI-LY3, OCI-LY10, U2932, and SUDHL2) and GCB-DLBCL cell lines (SUDHL1, SUDHL4, SUDHL5, SUDHL6, SUDHL8, SUDHL10, DB, RL, Toledo, WSU-NHL, RCK8, OCI-LY8, OCI-LY19, and HT) were used in this study. Relative gene expression of *PIM1*, *PIM2*, and *PIM3* was normalized to *GAPDH* by quantitative reverse transcription polymerase chain reaction (qRT-PCR). B. To confirm ibrutinib resistance, cells were treated with indicated concentrations of ibrutinib or vehicle for 3 days, and drug effect on cell growth was determined by CellTiter-Glo Luminescent Cell Viability Assay. C. *PIM1* was significantly increased in the ibrutinib-resistant TMD8 cells compared with the parental TMD8 cells from microarray analyses. D. Higher gene expression levels of *PIM1/2/3* in the ibrutinib-resistant TMD8 cells was confirmed by qRT-PCR. E. Higher PIM1 protein expression was identified in ibrutinib-resistant (ibR) TMD8 and HBL1 cells compared with parental (P) cells.

PIM1 mutations affected gene expression levels of upstream regulators and downstream targets of NF-κB

Given that ABC-DLBCL cells rely on NF-κB signaling for survival [25] and considering the potential role of PIM1 in NF-κB regulation [26], we explored the effect of PIM1 mutations on the expression levels of upstream regulators and downstream targets of the NF-κB pathway. We detected increased gene expression of a subset of NF-κB targets (*STAT1*, *CCL11*, *CCL5*, *IL1B*, *MMP9*) in the mutant PIM1-expressing TMD8 cells, whereas another subset of NF-κB targets (*ADM*, *CXCL1*, *CXCL2*, *EGFR*, *EGR2*, *IFNG*, *PDGFB*, *STAT5B*, *CCND1*) had decreased

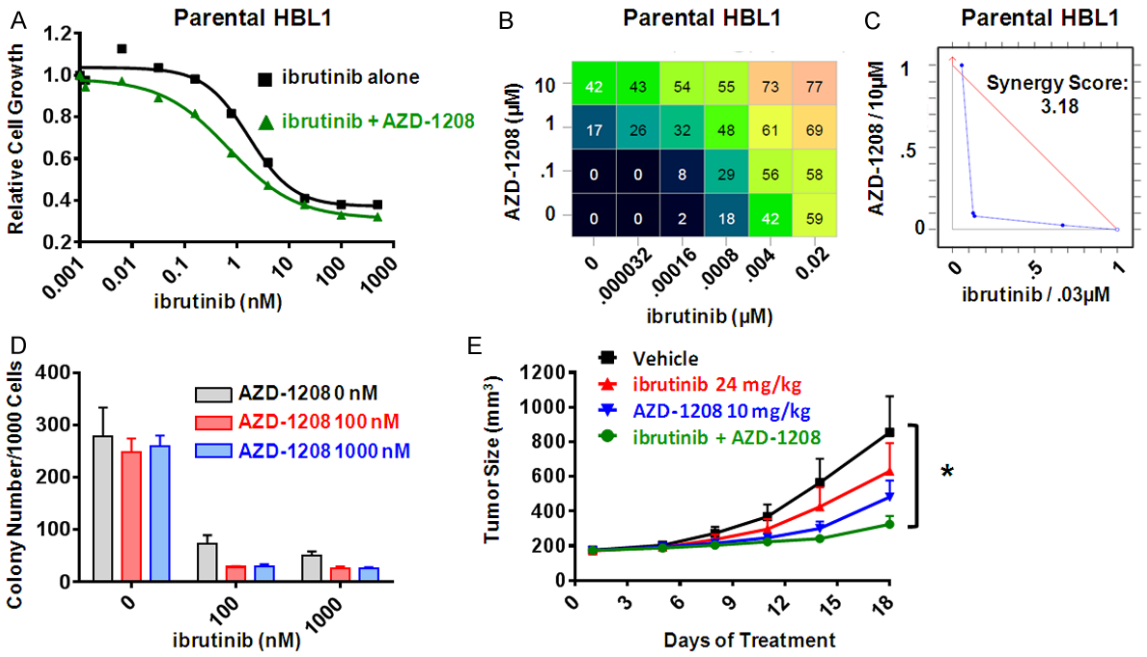

Figure 5. The combination of ibrutinib and AZD-1208 synergistically suppressed cell growth and reduced both colony formation and tumor growth. (A) Parental HBL1 cells were treated with indicated concentrations of ibrutinib combined with AZD-1208 (1,000 nM) or vehicle for 3 days, and drug effect on cell growth was determined by CellTiter-Glo Luminescent Cell Viability Assay. (B) Drug dose matrix data of parental HBL1 cells. The numbers indicate the percentage of growth inhibition of cells treated with the corresponding compound combination relative to vehicle control-treated cells. The data were visualized over the matrix using a color scale. (C) Isobologram analysis and synergy scores of the data in (B). (D) HBL1 cells were plated in 0.9% MethoCult (1,000 cells/well) with vehicle, ibrutinib (100 or 1,000 nM), AZD-1208 (100 or 1,000 nM), or the combinations, and colony formation was scored after 7 days. Graphs represent quantifications of 3 wells, expressed as mean ± SD. (E) HBL1 tumor cells were implanted into CB17 SCID mice, and the indicated drugs were orally administered daily when the tumors reached 150 mm^3. Tumors were measured twice a week. Significant tumor suppression was observed in the group treated with the ibrutinib/AZD-1208 combination compared with the vehicle-treated group (*P<0.01, repeated measures MANOVA-adjusted univariate F-test).

expression in mutant PIM1 cells (**Figure 3A** and **3B**). Among the upstream regulators of NF-κB, gene expression of *TLR4*, *TLR7*, and *IL1R1* was increased and gene expression of *TNFRSF11A*, *CD40*, and *TNFSF11* was decreased in the mutant *PIM1*-transduced TMD8 cells (**Figure 3C-F**). Expression of transcripts encoding proteins of the KEGG Toll-like receptor signaling pathway (M3261) and the BIOCARTA IL1R pathway (M12095) was enriched in mutant *PIM1*-transduced TMD8 cells compared with WT *PIM1*-transduced TMD8 cells (**Figure 3G** and **3H**), suggesting PIM1 mutations may play a role in enhancing specific upstream signaling of NF-κB, such as TLR4/7 and IL1R. Consistent with our *in vitro* results, clinical pretreatment FFPE specimens from the patients who experienced poor responses to ibrutinib (PD + SD) had higher expression of *TLR4*, *IL1R1*, and *IL1B* (**Figure 3I-K**).

Ibrutinib-resistant ABC-DLBCL cells had higher PIM1 expression

ABC-DLBCL cell lines had higher gene expression levels of all three PIM family members (*PIM1*, *PIM2*, and *PIM3*) compared with GCB-DLBCL cell lines, suggesting the potential role of PIM in the growth of ABC-DLBCL cells (**Figure 4A**). To understand whether PIM kinases could contribute to the development of acquired ibrutinib resistance, we selected TMD8 cells for resistance to ibrutinib by exposure to an escalating dose of the drug (**Figure 4B**, left). Intriguingly, microarray results that profiled gene expression revealed a strong upregulation of *PIM1* (approximately 15-fold) in ibrutinib-resistant TMD8 cells compared with parental cells (**Figure 4C**). Subsequent targeted gene expression profiling demonstrated that all three PIM family kinases are upregulated in ibrutinib-

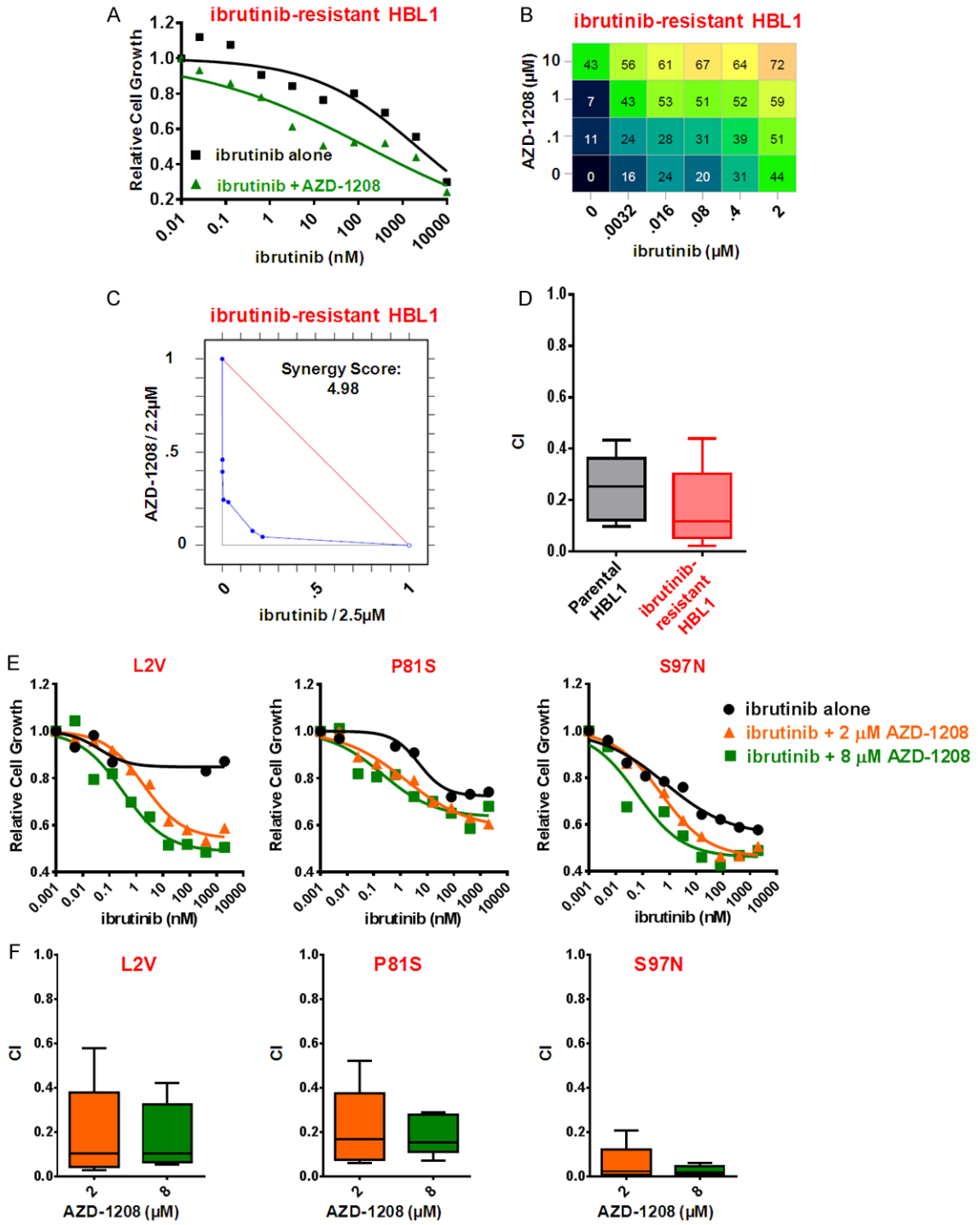

Figure 6. The combination of ibrutinib and AZD-1208 synergistically suppressed cell growth in ibrutinib-resistant and mutant PIM1-expressing cells. (A) Ibrutinib-resistant HBL1 cells were treated with the indicated concentrations of ibrutinib combined with AZD-1208 (1,000 nM) or vehicle for 3 days, and drug effect on cell growth was determined as in (A). (B) Drug dose matrix data of ibrutinib-resistant HBL1 cells. (C) Isobologram analysis and synergy scores of the data are shown in (B). (D) CI of ibrutinib and AZD-1208 combination in parental HBL1 and ibrutinib-resistant HBL1 cells. The CIs of different concentrations of ibrutinib combined with 1,000 nM AZD-1208 are shown. (E) Mutant *PIM1*-transduced TMD8 cells were treated with the indicated concentrations of ibrutinib combined with AZD-1208 (2 or 8 μM) or vehicle for 3 days, and drug effect on cell growth was determined. (F) CI of ibrutinib and AZD-1208 combination in mutant PIM1-transduced TMD8 cells. The CIs of different concentrations of ibrutinib combined with AZD-1208 at indicated concentrations is shown.

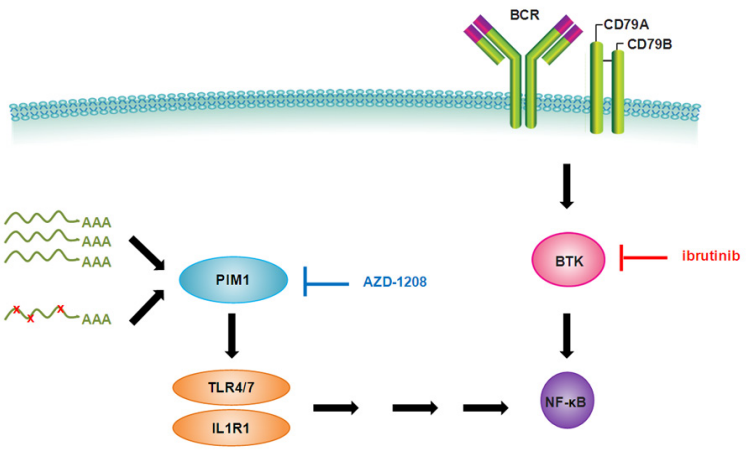

Figure 7. Hypothetical model of ibrutinib in combination with a PIM inhibitor in ABC-DLBCL cells. Upregulation of gene expression and protein stabilization induced by mutations contribute to the increased protein level of PIM1, which further controls upstream regulators of NF-κB, such as TLR4/7 and IL1R1. In the ibrutinib-resistant cells, combined inhibition of BTK and PIM1 may provide better efficacy.

resistant TMD8 cells (**Figure 4D**). In addition, we confirmed that PIM1 protein is upregulated in both TMD8 and HBL1 cells selected for ibrutinib resistance (**Figure 4B** and **4E**).

The combination of ibrutinib and AZD-1208 synergistically suppressed cell growth and reduced colony formation and tumor growth of ABC-DLBCL cells

Because we demonstrated that gain-of-function PIM1 mutations might contribute to ibrutinib resistance, we hypothesized that the combined inhibition of PIM kinases and BTK may potentially be effective for ABC-DLBCL treatments. Therefore, we tested the combination of ibrutinib and a pan-PIM inhibitor, AZD-1208, in parental HBL1 cells and identified moderate synergy between the two compounds (**Figure 5A-C**). Addition of AZD-1208 further decreased colony formation of HBL1 cells beyond single-agent ibrutinib treatment (**Figure 5D**). As further confirmation, we injected HBL1 cells into CB17 SCID mice to form tumor xenografts. Treatment with either ibrutinib or AZD-1208 as a single agent partially delayed tumor growth. Combined dosing, however, almost completely halted growth for the duration of treatment (**Figure 5E**). We also tested this combination in ibrutinib-resistant HBL1 cells and again found that the combination was moderately synergistic (**Figure 6A-D**). Finally, we investigated whether AZD-1208 could overcome ibrutinib resistance in TMD8 cells expressing mutant PIM1. We found that although each of the three mutant PIM1-expressing lines was largely resistant to ibrutinib alone, addition of AZD-1208 sensitized these lines to ibrutinib (**Figure 6E** and **6F**), further confirming that PIM kinase activity is sufficient to induce ibrutinib resistance in ABC-DLBCL cell lines.

Discussion

Ibrutinib has shown significant efficacy in a subset of ABC-DLBCL [8]. However, additional work is required to differentiate patient populations regarding their response to ibrutinib. In this report, we describe novel mutations in PIM1 that were identified in ABC-DLBCL patients with a poor response to ibrutinib. Introduction of these PIM1 mutations into ABC-DLBCL cell lines reduced their sensitivity to ibrutinib. Transduction of mutant *PIM1* into ABC-DLBCL cells resulted in increased colony formation without affecting cell growth or viability compared with transduction of WT *PIM1*. Because of the critical role of NF-κB in ABC-DLBCL, we further investigated the effect of PIM1 mutations on NF-κB signaling. Upregulation of NF-κB upstream regulators TLR4/7 and IL1R1 was identified in the mutant PIM1-expressing cells. This result was consistent with our findings that ABC-DLBCL patients with poorer responses to ibrutinib had higher gene expression levels of TLR4, IL1R1, and IL1B. In addition, expression of a subset of NF-κB target genes was enhanced in ABC-DLBCL cells containing mutant PIM1. Conceptually, this finding agrees with previous reports that reactivation of NF-κB by a mutation in *PLCG2* can result in acquired resistance to ibrutinib [27]. PIM family kinases have been linked to survival and proliferation in ABC-DLBCL and to regulation of mTOR signaling [17, 24]. In addition, PIM1 is an upstream regulator of NF-κB signaling [26, 28]. Therefore, PIM1 mutations may serve to enhance ABC-DLBCL tumorigenesis as well as elicit resistance to ibrutinib. Taken together with previous studies, these findings highlight the necessity to understand the genetic background of DLBCL and

other B cell lymphomas when determining an appropriate therapeutic option.

All 3 mutations in PIM1 induced similar effects on NF-κB signaling, ibrutinib sensitivity, and clonogenicity despite differences in mutation site. Only 2 of the identified mutations are located in the kinase domain. Previous studies revealed decreased kinase activity in several PIM1 variants [29], and overexpression of a kinase-dead PIM1 mutant resulted in the formation of larger tumors, suggesting that kinase-independent functions of PIM1 may play a role in oncogenesis. In contrast with other protein kinases, PIM1 is constitutively active and its activity is regulated by its expression level and stability [30]. The PIM1 mutations we identified in patients with poor ibrutinib responses appeared to increase PIM1 protein stability. In addition, gene and protein expression levels were upregulated in the ibrutinib-resistant ABC-DLBCL cells generated by drug treatment compared with parental cells. These results suggest that the PIM1 protein level can be increased by 2 potential mechanisms (WT *PIM1* gene upregulation or increased mutant PIM1 protein half-life).

Collectively, our data implicate a role of PIM1 in ibrutinib resistance, either through mutation or increased gene expression, and suggest that disruption of this mechanism may improve ibrutinib efficacy (**Figure 7**). We showed that the combination of a pan-PIM inhibitor with ibrutinib can overcome resistance induced both by expression of PIM1 mutants or by prolonged drug treatment. Based on our findings in both *in vitro* and *in vivo* models, the dual targeting of BTK and PIM kinases in ABC-DLBCL may both enhance drug response and prevent acquisition of resistance.

Acknowledgements

Brian Haas, PhD, of Nexus GG Science, a medical writer supported by funding from Pharmacyclics, LLC, an AbbVie Company, provided editorial assistance to the authors during preparation of this manuscript. We thank Xuan Ma and Joseph Cefalu for helping with animal experiments.

Disclosure of conflict of interest

HPK, KE, BYC: employment and patents with Pharmacyclics, LLC, an AbbVie Company, stock from AbbVie; MS: employment with Pharmacyclics, LLC, an AbbVie Company, stock from AbbVie; SAE: employment with AbbVie, employment with St. Francis Hospital (spouse), stock from AbbVie, travel, accommodations, or expenses covered by AstraZeneca and Amgen; SH: employment with Pharmacyclics, LLC, an AbbVie Company; KJS: employment, stock, and patents with Pharmacyclics, LLC, an AbbVie Company, employment and stock from AbbVie; LWKC: employment and patents with Pharmacyclics, LLC, an AbbVie Company, stock from Eli Lilly & Co and AbbVie; SW: employment and patents pending with Pharmacyclics, LLC, an AbbVie Company, stock from AbbVie; MA: employment with Pharmacyclics, LLC, an AbbVie Company, equity ownership with AbbVie; YL: employment with Pharmacyclics, LLC, an AbbVie Company, stock from AbbVie; JH: employment with Pharmacyclics, LLC, an AbbVie Company, stock from AbbVie, employment with Astellas; CTC: employment with Pharmacyclics, LLC, an AbbVie Company and MD Anderson Cancer Center, research funding obtained from MD Anderson Cancer Center; DB: employment, leadership, patents, royalties, or other intellectual property, and travel with Pharmacyclics, LLC, an AbbVie Company, equity ownership with AbbVie.

Address correspondence to: Betty Y Chang, Department of Research, Pharmacyclics LLC, an AbbVie Company, 995 E. Arques Avenue, Sunnyvale, CA 94085, USA. Tel: 408-215-3358; Fax: 408-215-3358; E-mail: bchang@pcyc.com

References

[1] Tsukada S, Saffran DC, Rawlings DJ, Parolini O, Allen RC, Klisak I, Sparkes RS, Kubagawa H, Mohandas T, Quan S, Belmont JW, Cooper MD, Conley ME, Witte ON. Deficient expression of a B cell cytoplasmic tyrosine kinase in human X-linked agammaglobulinemia. Cell 1993; 72: 279-290.

[2] Davis RE, Ngo VN, Lenz G, Tolar P, Young RM, Romesser PB, Kohlhammer H, Lamy L, Zhao H, Yang Y, Xu W, Shaffer AL, Wright G, Xiao W, Powell J, Jiang JK, Thomas CJ, Rosenwald A, Ott G, Muller-Hermelink HK, Gascoyne RD, Connors JM, Johnson NA, Rimsza LM, Campo E, Jaffe ES, Wilson WH, Delabie J, Smeland EB, Fisher RI, Braziel RM, Tubbs RR, Cook JR, Weisenburger DD, Chan WC, Pierce SK and Staudt LM. Chronic active B-cell-receptor signalling in diffuse large B-cell lymphoma. Nature 2010; 463: 88-92.

[3] Herman SE, Gordon AL, Hertlein E, Ramanunni A, Zhang X, Jaglowski S, Flynn J, Jones J, Blum KA, Buggy JJ, Hamdy A, Johnson AJ and Byrd JC. Bruton tyrosine kinase represents a promising therapeutic target for treatment of chronic lymphocytic leukemia and is effectively targeted by PCI-32765. Blood 2011; 117: 6287-6296.

[4] Irish JM, Czerwinski DK, Nolan GP and Levy R. Altered B-cell receptor signaling kinetics distinguish human follicular lymphoma B cells from tumor-infiltrating nonmalignant B cells. Blood 2006; 108: 3135-3142.

[5] Cinar M, Hamedani F, Mo Z, Cinar B, Amin HM and Alkan S. Bruton tyrosine kinase is commonly overexpressed in mantle cell lymphoma and its attenuation by Ibrutinib induces apoptosis. Leuk Res 2013; 37: 1271-1277.

[6] Honigberg LA, Smith AM, Sirisawad M, Verner E, Loury D, Chang B, Li S, Pan Z, Thamm DH, Miller RA and Buggy JJ. The Bruton tyrosine kinase inhibitor PCI-32765 blocks B-cell activation and is efficacious in models of autoimmune disease and B-cell malignancy. Proc Natl Acad Sci U S A 2010; 107: 13075-13080.

[7] Herman SE, Mustafa RZ, Gyamfi JA, Pittaluga S, Chang S, Chang B, Farooqui M and Wiestner A. Ibrutinib inhibits BCR and NF-kappaB signaling and reduces tumor proliferation in tissue-resident cells of patients with CLL. Blood 2014; 123: 3286-3295.

[8] Wilson WH, Young RM, Schmitz R, Yang Y, Pittaluga S, Wright G, Lih CJ, Williams PM, Shaffer AL, Gerecitano J, de Vos S, Goy A, Kenkre VP, Barr PM, Blum KA, Shustov A, Advani R, Fowler NH, Vose JM, Elstrom RL, Habermann TM, Barrientos JC, McGreivy J, Fardis M, Chang BY, Clow F, Munneke B, Moussa D, Beaupre DM and Staudt LM. Targeting B cell receptor signaling with ibrutinib in diffuse large B cell lymphoma. Nat Med 2015; 21: 922-926.

[9] Alvarado Y, Giles FJ and Swords RT. The PIM kinases in hematological cancers. Expert Rev Hematol 2012; 5: 81-96.

[10] Dhanasekaran SM, Barrette TR, Ghosh D, Shah R, Varambally S, Kurachi K, Pienta KJ, Rubin MA and Chinnaiyan AM. Delineation of prognostic biomarkers in prostate cancer. Nature 2001; 412: 822-826.

[11] Brault L, Gasser C, Bracher F, Huber K, Knapp S and Schwaller J. PIM serine/threonine kinases in the pathogenesis and therapy of hematologic malignancies and solid cancers. Haematologica 2010; 95: 1004-1015.

[12] Amson R, Sigaux F, Przedborski S, Flandrin G, Givol D and Telerman A. The human protooncogene product p33pim is expressed during fetal hematopoiesis and in diverse leukemias. Proc Natl Acad Sci U S A 1989; 86: 8857-8861.

[13] Hsi ED, Jung SH, Lai R, Johnson JL, Cook JR, Jones D, Devos S, Cheson BD, Damon LE and Said J. Ki67 and PIM1 expression predict outcome in mantle cell lymphoma treated with high dose therapy, stem cell transplantation and rituximab: a Cancer and Leukemia Group B 59909 correlative science study. Leuk Lymphoma 2008; 49: 2081-2090.

[14] Mahadevan D, Spier C, Della Croce K, Miller S, George B, Riley C, Warner S, Grogan TM and Miller TP. Transcript profiling in peripheral T-cell lymphoma, not otherwise specified, and diffuse large B-cell lymphoma identifies distinct tumor profile signatures. Mol Cancer Ther 2005; 4: 1867-1879.

[15] Merkel AL, Meggers E and Ocker M. PIM1 kinase as a target for cancer therapy. Expert Opin Investig Drugs 2012; 21: 425-436.

[16] Zhang F, Beharry ZM, Harris TE, Lilly MB, Smith CD, Mahajan S and Kraft AS. PIM1 protein kinase regulates PRAS40 phosphorylation and mTOR activity in FDCP1 cells. Cancer Biol Ther 2009; 8: 846-853.

[17] Gomez-Abad C, Pisonero H, Blanco-Aparicio C, Roncador G, Gonzalez-Menchen A, Martinez-Climent JA, Mata E, Rodriguez ME, Munoz-Gonzalez G, Sanchez-Beato M, Leal JF, Bischoff JR and Piris MA. PIM2 inhibition as a rational therapeutic approach in B-cell lymphoma. Blood 2011; 118: 5517-5527.

[18] Keeton EK, McEachern K, Dillman KS, Palakurthi S, Cao Y, Grondine MR, Kaur S, Wang S, Chen Y, Wu A, Shen M, Gibbons FD, Lamb ML, Zheng X, Stone RM, Deangelo DJ, Platanias LC, Dakin LA, Chen H, Lyne PD and Huszar D. AZD1208, a potent and selective pan-Pim kinase inhibitor, demonstrates efficacy in preclinical models of acute myeloid leukemia. Blood 2014; 123: 905-913.

[19] Chou TC and Talalay P. Quantitative analysis of dose-effect relationships: the combined effects of multiple drugs or enzyme inhibitors. Adv Enzyme Regul 1984; 22: 27-55.

[20] Ling X, Westover D, Cao F, Cao S, He X, Kim HR, Zhang Y, Chan DC and Li F. Synergistic effect of allyl isothiocyanate (AITC) on cisplatin efficacy in vitro and in vivo. Am J Cancer Res 2015; 5: 2516-2530.

[21] Zhang X, Ma Y, Wei H, Li B, Xiao F, Yang J, Yue Q, Yang A and Hao X. A prostate-specific antigen-dependent fusion polypeptide inhibits growth of prostate cancer cells in vitro and in vivo. Am J Cancer Res 2016; 6: 1053-1065.

[22] Wright G, Tan B, Rosenwald A, Hurt EH, Wiestner A and Staudt LM. A gene expression-based method to diagnose clinically distinct subgroups of diffuse large B cell lymphoma. Proc Natl Acad Sci U S A 2003; 100: 9991-9996.

[23] Frampton GM, Fichtenholtz A, Otto GA, Wang K, Downing SR, He J, Schnall-Levin M, White J,

Sanford EM, An P, Sun J, Juhn F, Brennan K, Iwanik K, Maillet A, Buell J, White E, Zhao M, Balasubramanian S, Terzic S, Richards T, Banning V, Garcia L, Mahoney K, Zwirko Z, Donahue A, Beltran H, Mosquera JM, Rubin MA, Dogan S, Hedvat CV, Berger MF, Pusztai L, Lechner M, Boshoff C, Jarosz M, Vietz C, Parker A, Miller VA, Ross JS, Curran J, Cronin MT, Stephens PJ, Lipson D and Yelensky R. Development and validation of a clinical cancer genomic profiling test based on massively parallel DNA sequencing. Nat Biotechnol 2013; 31: 1023-1031.

[24] Brault L, Menter T, Obermann EC, Knapp S, Thommen S, Schwaller J and Tzankov A. PIM kinases are progression markers and emerging therapeutic targets in diffuse large B-cell lymphoma. Br J Cancer 2012; 107: 491-500.

[25] Young RM, Shaffer AL 3rd, Phelan JD and Staudt LM. B-cell receptor signaling in diffuse large B-cell lymphoma. Semin Hematol 2015; 52: 77-85.

[26] Nihira K, Ando Y, Yamaguchi T, Kagami Y, Miki Y and Yoshida K. Pim-1 controls NF-kappaB signalling by stabilizing RelA/p65. Cell Death Differ 2010; 17: 689-698.

[27] Liu TM, Woyach JA, Zhong Y, Lozanski A, Lozanski G, Dong S, Strattan E, Lehman A, Zhang X, Jones JA, Flynn J, Andritsos LA, Maddocks K, Jaglowski SM, Blum KA, Byrd JC, Dubovsky JA and Johnson AJ. Hypermorphic mutation of phospholipase C, gamma2 acquired in ibrutinib-resistant CLL confers BTK independency upon B-cell receptor activation. Blood 2015; 126: 61-68.

[28] Kim K, Kim JH, Youn BU, Jin HM and Kim N. Pim-1 regulates RANKL-induced osteoclastogenesis via NF-kappaB activation and NFATc1 induction. J Immunol 2010; 185: 7460-7466.

[29] Kumar A, Mandiyan V, Suzuki Y, Zhang C, Rice J, Tsai J, Artis DR, Ibrahim P and Bremer R. Crystal structures of proto-oncogene kinase Pim1: a target of aberrant somatic hypermutations in diffuse large cell lymphoma. J Mol Biol 2005; 348: 183-193.

[30] Qian KC, Wang L, Hickey ER, Studts J, Barringer K, Peng C, Kronkaitis A, Li J, White A, Mische S and Farmer B. Structural basis of constitutive activity and a unique nucleotide binding mode of human Pim-1 kinase. J Biol Chem 2005; 280: 6130-6137.